ANALYTICAL MODEL TO PREDICT FAILURE OF WOVEN COMPOSITES

S. T. Pinho[1]*, N. V. De Carvalho[1], P. Robinson[1]
[1] Dep. of Aeronautics, Imperial College London, London, UK
* Corresponding author (silvestre.pinho@imperial.ac.uk)

Keywords: *Woven Composites, Failure, Finite Element Modelling*

1 Introduction

Various analytical models have been proposed, with different degrees of complexity, e.g. [1-7]. The meso-scale models from Tan et al. [6] and Naik et al. [7], proposed for plain weave composites, are worth highlighting, as they share a similar approach to the one proposed herein. Both models are based on a beam on elastic foundation formulation. The load-aligned tow is considered to be an UD composite, and modelled as an Euler-Bernoulli beam. Tan et al. [6] focuses on predicting tensile failure. The authors assume the load-aligned tow has a sinusoidal shape. The elastic foundation is introduced to model the supporting effect of the matrix; the support provided by the transverse tows, as well the effect of the presence of adjacent layers (on the through-thickness direction), are neglected. Results show the proposed model over-predicts the tensile strength.

Naik et al. [7] presents a refined formulation and applies it to predict the compressive failure strength. The authors discretise the beam in several elements and calculate the elastic foundation stiffness and the load distribution for each element. The contributions of matrix and transverse tows to the elastic foundation are both accounted for. Additionally, they also account for the support provided by the adjacent layers by considering two different cases of shifting between adjacent plies. Results show the model over-predicts compressive failure strength.

Both approaches [6,7] calculate the elastic foundation stiffness in a semi-empirical fashion, considering that the elastic foundation provides normal support only, and neglecting the weave effect, i.e. the effect of the deflection of the adjacent in-plane tows.

Recent experimental evidence has highlighted the behaviour of tows as structural elements at the reinforcement level [8]. It was observed that the support provided by the adjacent layers affects the damage mechanisms and that damage morphology, at both lamina and laminate level, is affected by the weave architecture and geometry [8]. Therefore, in order to capture the physics of the failure of this type of materials, it is necessary to: (i) model the beam-like behaviour of the load-aligned tows, (ii) account for the relative shift between adjacent layers in the support provided to each layer, (iii) explicitly model the weave architecture and/or its effect.

Following the work from Tan et al. [6] and Naik et al. [7], the proposed approach is based on a beam on elastic foundation formulation. Two practical bounds for the support provided by the adjacent layers are considered: In-Phase (IP) and Out-of-Phase (OP). The elastic foundation is considered to provide not only normal support, but also torsional support to the load-aligned tow. The constants of the elastic foundation are physically derived, and depend upon: (i) through-thickness support provided by the adjacent layers being considered (IP or OP), (ii) weave effect, and (iii) properties of both matrix and transverse tow. To assist the validation of the analytical model, an equivalent numerical model was developed. Numerical and analytical results for the local stresses along the load-aligned tow are compared. Finally, the constitutive response and final failure predicted analytically is compared to experimental results obtained for uniaxial tension and compression of a 2×2 twill carbon-epoxy composite and conclusions are drawn.

2 Analytical Model

The analytical model consists of an Euler-Bernoulli beam under axial tension/compression on an elastic foundation. The beam represents the load-aligned tow and is regarded as an UD composite. The elastic foundation provides normal and torsional support.

As referred previously, the properties of the elastic foundation are physically derived, and are a function of: weave pattern, support provided by the adjacent layers and properties of matrix/transverse tows. The present section provides a brief summary of the main features of the model presented. Further details can be found in [9].

2.1 Geometry

Exploiting existing symmetries, it is possible to define a 2D representative model of a 2×2 twill weave consisting of half a sinusoidal beam connected with a straight beam, regions A and B of **Figure 1**.

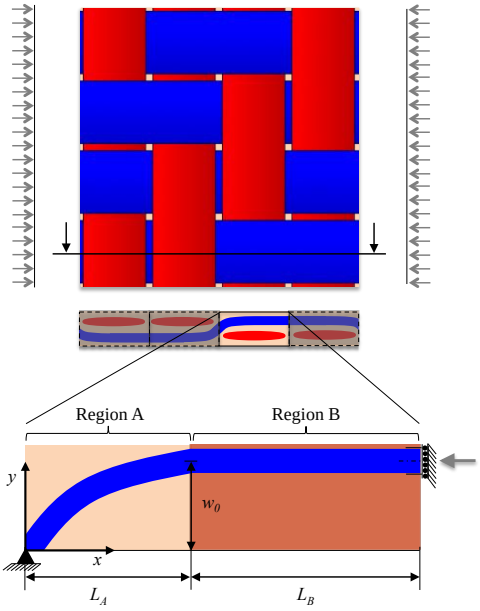

Figure 1. Geometry of the analytical model for a 2×2 twill weave.

2.2 Weave pattern

The weave pattern affects the response of the woven composite under loading. In-plane adjacent tows affect the deflection of each other through the shearing of the matrix connecting them, Figure 2. The shear strain of the matrix connecting two adjacent tows can be estimated by relating the deflection of each tow. Knowing the shear strain, the pressure exerted by the adjacent tows can be approximated by:

$$p_{weave} = \frac{(2w_0+2\overline{t_{tow}})G_m w(x)}{g}, \quad (1)$$

where w_0 is a geometrical parameter, defined in Figure 1, $\overline{t_{tow}}$ represents the average tow thickness (the cross section of the tows is assumed to be elliptical), G_m is the shear modulus of the matrix, g is the gap between adjacent tows, and $w(x)$ the vertical displacement of a load aligned tow.

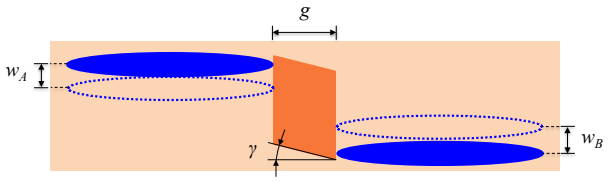

Figure 2. Shearing of the matrix connecting two adjacent tows (in-plane).

2.3 Through-thickness support

2.3.1 In-Phase (IP)

In the IP case, the support provided to the tow by the adjacent layers is essentially given by: (i) the shearing of the material between load-aligned tows of adjacent layers, and (ii) the pressure that originates from the gradient of that shearing stress.

Upon loading, the rotation of tows in an IP laminate causes the region between adjacent tows to shear, Figure 3. Analysing the kinematic model of Figure 3, it is possible to derive an expression for the shear stress applied to the tow:

$$\tau_{IP} = G_h\left(1+\frac{\overline{t_{tow}}}{\overline{h_{Layer}}}\right)\frac{dw}{dx}, \quad (2)$$

where G_h is the homogenized modulus of the region between load-aligned tows of adjacent layers and $\overline{h_{Layer}}$ is the average vertical length of that region. Analysing the vertical equilibrium of the region between tows, Figure 4, it comes that the gradient of the shear stress induces a normal pressure applied to the tow given by:

$$p_{d\tau/dx} = -\frac{d\tau}{dx}\overline{h_{Layer}}b_{tow}, \quad (3)$$

where b_{tow} is the width of the cross-section of the tow.

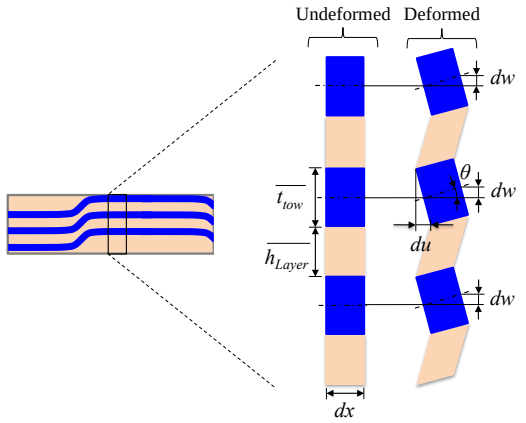

Figure 3. Kinematic model illustrating the shearing of the material between load-aligned tows of adjacent layers upon loading in an IP laminate.

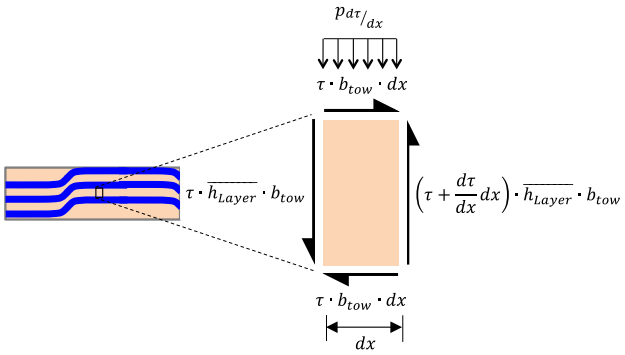

Figure 4. Equilibrium of an element of the region between load-aligned tows of adjacent layers.

2.3.1 Out-of-Phase (OP)

In the OP case, the support is essentially provided by: (i) a direct pressure applied by the load-aligned tows of adjacent layers, resulting from their displacement in opposite directions, and (ii) the shearing of the material between the load-aligned tows of adjacent layers. Both effects can be derived form the kinematic model of Figure 5. Similarly to the IP case, upon loading the regions between the tows will shear. The analysis of the kinematic model results in the following expression for the shear stress applied to the tow:

$$\tau_{OP} = G_h \frac{dw}{dx} \tag{4}$$

Figure 5 shows that adjacent tows displace identically but in opposite directions. The latter leads to a direct pressure being applied that can be estimated by:

$$p_{adj} = 2w(x)\left(\frac{E_{h-Top}(1-\nu_{h-Top})}{\overline{h_{Top}}(1+\nu_{h-Top})(1-2\nu_{h-Top})} + \frac{E_{h-Bot}(1-\nu_{h-Bot})}{\overline{h_{Bot}}(1+\nu_{h-Bot})(1-2\nu_{h-Bot})}\right), \tag{5}$$

where $E_{h-Top/Bot}$ and $\nu_{h-Top/Bot}$ are the homogenised stiffness and Poisson's ratio of the regions between a given tow and the top and bottom adjacent tows. The variables $\overline{h_{Top/Bot}}$ are the vertical distances between a given tow and the top and bottom adjacent tows, Figure 5.

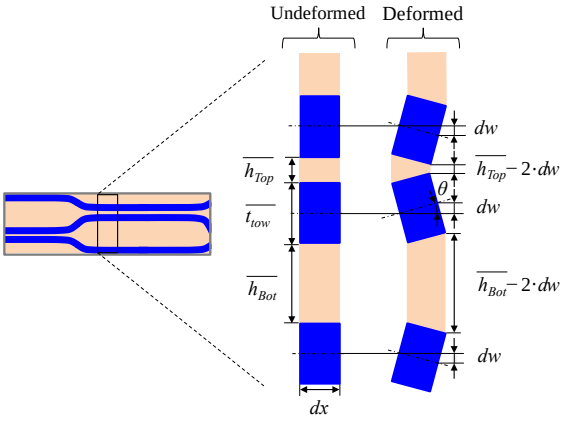

Figure 5. Kinematic model illustrating the local shearing of the material between load-aligned tows upon loading and the displacement of adjacent tows in opposite directions in an OP laminate.

2.4 Beam Equilibrium and Differential Equation

Having identified all relevant features, the differential equation is derived from the equilibrium of an infinitesimal element of the beam, Figure 6. The loads applied are: axial load P (tension or compression), a pressure per unit length $p(x)$ and a shear stress $\tau(x)$. As highlighted previously, the different cases of through-thickness support, IP and OP, lead to different expressions for the shear and pressure applied to the tow. Using Eqs (1) to (5) and after some manipulation, it is possible to arrive to the following differential equation:

$$\frac{d^4w}{dx^4} + \lambda_1^2 \frac{d^2w}{dx^2} + \lambda_2^2 w = -\lambda_3^2 \frac{d^2w_0}{dx^2} \tag{6}$$

where the constants, λ_1, λ_2 and λ_3 are a function of the case of support being considered, IP or OP; further details are provided in [9].

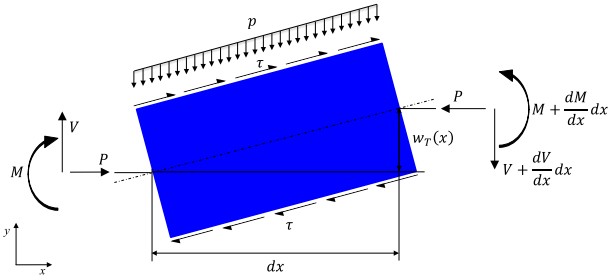

Figure 6. Equilibrium of an infinitesimal beam element.

2.5 Failure prediction

Compressive and tensile failure are predicted using two different failure criteria: maximum stress and physically-based criteria [10]. Both set of criteria are applied at the tow level. The material is assumed to fail after failure of the tows is detected using one of the referred criteria. The maximum stress criteria compare directly the measured strengths of a given material with the applied stresses. The physically-based criteria consider different failure modes separately and the equations used to predict each failure mode are derived from the physics of the failure process. Longitudinal compressive failure of the tows is predicted using a kinking criterion [10]:

$$FI_{KINK} = \left(\frac{\tau_{23}^m}{S_T - \eta_T \sigma_2^m}\right)^2 + \left(\frac{\tau_{12}^m}{S_L - \eta_L \sigma_2^m}\right)^2 + \left(\frac{\langle \sigma_2^m \rangle_+}{Y_T}\right) = 1 \quad (7)$$

To predict tensile failure a maximum stress criterion is used, as it is shown to correlate well with existing experimental data.

3 Finite Element Model - reduced Unit Cell

3.1 Geometry, mesh & properties

The numerical model developed consists of a reduced Unit Cell (rUC) of a 2×2 twill weave, Figure 7. It corresponds to the nominal geometry of the carbon-epoxy composite characterized in [8]. The model was developed and solved in Abaqus/Standard. The section of the tows is assumed to have an elliptical shape, and the path of the tows is defined using a spline interpolation. In order to capture accurately the bending response of the tows, six elements were used in the through-thickness direction. They are assumed to consist of an orthotropic material, with the material orientations following the central path of the tow. The matrix was modelled as an isotropic material. Material properties for tows and matrix were obtained from [11] and [12], respectively.

3.2 Boundary conditions and loading

Periodic Boundary Conditions (PBC) were applied to the rUC using the formulation developed in [13]. Symmetries within the UC are exploited enabling the reduction of the analysis domain to 1/16th of the UC, whilst guaranteeing the same response is obtained. Details on how to apply PBCs to this particular rUC are provided in [13]. In the through-thickness direction, PBCs are applied to represent two types of laminates: In-Phase (IP) and Out-of-Phase (OP). Two cases of loading are considered: uniaxial tension and compression. The model was solved using large displacements formulation.

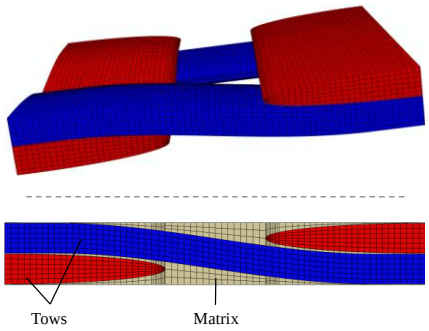

Figure 7. Finite element model of the 2×2 twill rUC used.

4 Results

4.1 Mesoscale stress comparison

Numerical and analytical results show, in general, good agreement. The analytical model developed captures well the difference in response between IP and OP cases, Figure 8a and Figure 8b. The range of stresses for all cases is well predicted as well as their local trends. Nevertheless, the numerical and experimental results for the IP case show a better agreement than for the OP. This is due to the significant decrease in the bending of the tows, and proportional increase in the effect of the local deformations of the material between tows of adjacent layers.

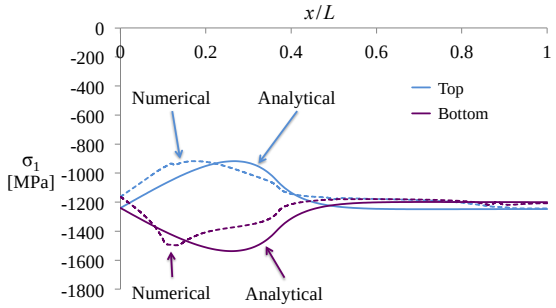

(a) IP

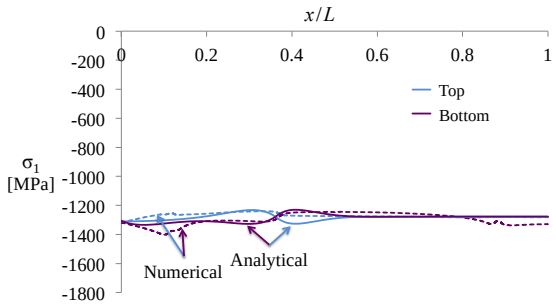

(b) OP

Figure 8. σ_1 determined along the tow and at the centre of the top and bottom surfaces. In both cases the tow is under a compressive strain of $\varepsilon_1 = -0.008$.

4.2 Constitutive response and failure prediction

In the tensile case, Figure 9a, the constitutive response is well captured apart from the slight stiffening verified experimentally. The latter is possibly due to the stiffening of the fibres [14] not represented in the model. Using a maximum stress criterion, the range of both failure strain and stress is slightly over-predicted. As expected, the failure stress predicted in the IP case is lower than that for the OP case, due to a decrease in the bending of the load-aligned tow. Averaging the stress predictions for the IP and OP cases, the failure stress is over-predicted by ~5%, Figure 10a. In the compression case, Figure 9b, the variability of the constitutive response is higher than for the tensile case. The analytical model captures well the stiffer constitutive responses, apart from the nonlinear region near failure. The latter leads to a slight under-prediction of the failure strains. As referred previously, two different sets of criteria were used to predict compressive failure: maximum stress and physically-based. Both have a similar failure prediction for the IP case. In the OP case, the physically-based failure criteria predict failure for higher stresses than the maximum stress criteria. Therefore, the physically-based failure criteria predict a wider range of failure stress and strains. Averaging the predictions for the two cases, IP and OP, the physically-based failure criteria and the maximum stress criteria under-predict the compressive strength by ~6% and 17%, respectively, Figure 10b. Finally, both in tension and compression, the effect of considering two different cases of support, IP and OP, is relatively more significant in the prediction of the failure stress than in the prediction of the constitutive response.

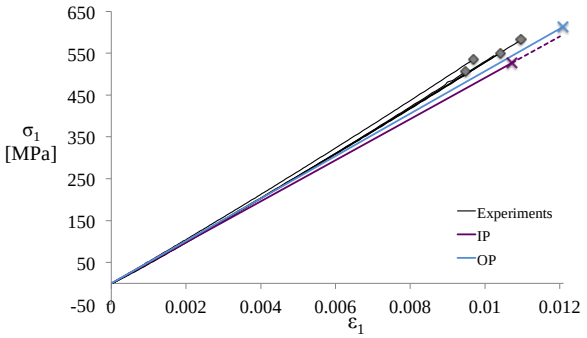

(a) Tension

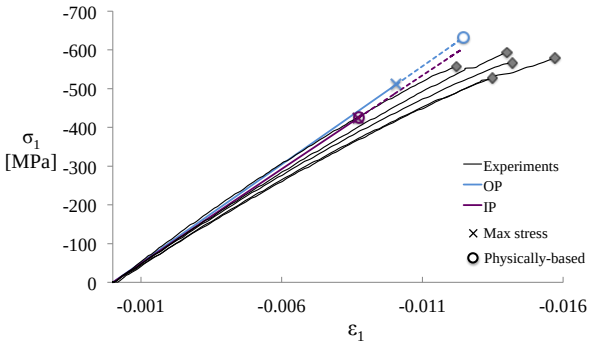

(b) Compression

Figure 9 Comparison between the constitutive responses predicted and obtained experimentally. Failure is determined using both maximum stress and physically-based failure criteria

5 Conclusions

An analytical model, based on a beam on elastic foundation, has been developed. The elastic foundation provides both normal and torsional

support. Its properties are physically derived and account for: i) weave effect, ii) support provided by the adjacent layers and iii) the properties of matrix and transverse tows. The local stress predictions obtained analytically compare well with the predictions made by an equivalent numerical model, both in terms of maximum/minimum stresses and local trends. This agreement guarantees the essential physics of the deformation process are well captured. The constitutive response predicted also shows good agreement with experiments. The discrepancies found are related with the nonlinear material response of the composite constituents near failure. The latter can be incorporated in the analytical model, albeit compromising its simplicity. The proposed model accurately predicts the tensile and compressive failure strengths, particularly when physically-based failure criteria are used. Additionally, it also enables the analytical determination of range values for the failure strengths, which are seen to agree well with the experimental data available.

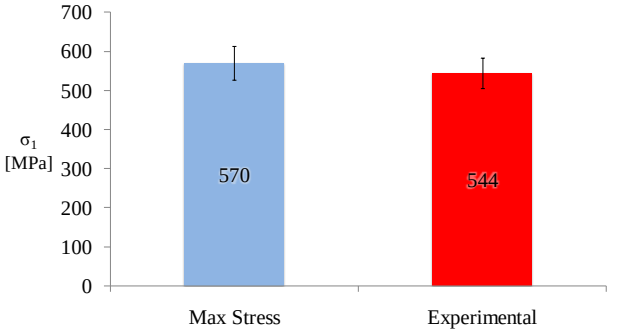

(a) Tension

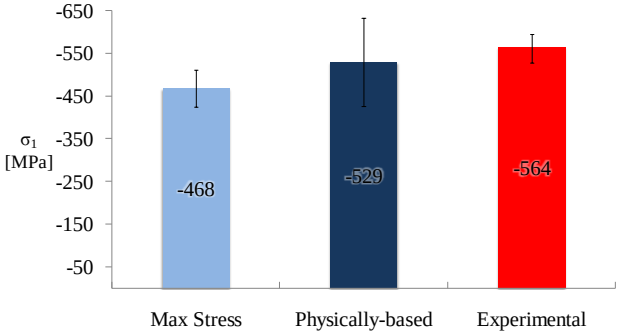

(b) Compression

Figure 10. Comparison between experimental and predicted failure strengths using maximum stress and physically-based failure criteria

References

[1] T. Ishikawa and T.W. Chou "Nonlinear behavior of woven fabric composites". *Journal of Composite Materials*, Vol. 17, pp 399-413, 1983.

[2] T. Ishikawa and T.W. Chou "Stiffness and strength behaviour of woven fabric composites". *Journal of Materials Science*, Vol. 17, pp 3211-3220, 1982.

[3] M. Karayaka and P. Kurath "Deformation and failure behavior of woven composite laminates". *Journal of Engineering Materials and Technology* Vol. 116, pp 222– 232, 1994.

[4] N.K. Naik and V.K. Ganesh "Failure behavior of plain of weave fabric laminates under on-axis uniaxial tensile loading: I-Analytical predictions". *Journal of Composite Materials*, Vol. 30, pp 1779-1822, 1996.

[5] F. Edgren and L.E. Asp "Approximate analytical constitutive model for non-crimp fabric composites." *Composites Part A: Applied Science and Manufacturing*, pp 173-181, 2005.

[6] P. Tan, L. Tong, and G.P. Steven "Micromechanics models for the elastic constants and failure strengths of plain weave composites". *Composite Structures*, Vol. 47, No 1-4, pp 797-804, 1999.

[7] N.K. Naik, S.I. Tiwari, and R.S. Kumar "An analytical model for compressive strength of plain weave fabric composites". *Composites Science and Technology*, Vol. 63, No 5, pp 609-625, 2003.

[8] N.V. de Carvalho, S.T. Pinho, P. Robinson "An experimental study of failure initiation and propagation in 2D woven composites under compression" *Composites Science and Technology*, In Press, 2010.

[9] N.V. de Carvalho, S.T. Pinho, P. Robinson "Analytical modelling of the compressive and tensile response of 2D woven composites". To be submitted, 2011.

[10] S.T. Pinho et al, "Material and structural response of polymer-matrix fibre-reinforced composites". *Composites Science and Technology*, accepted, 2008.

[11] McCarroll CA. "Material characterisation of T300/920". Technical report, Imperial College London, 2007.

[12] Hexply 920 product data sheet, 2007.

[13] N.V. de Carvalho, S.T. Pinho, P. Robinson "Reducing the domain in the mechanical analysis of periodic structures, with application to woven composites". *Composites Science and Technology* Vol. 71, No. 7, pp 969-979, 2011.

[14] S.V. Lomov, A.E. Bogdanovich, I. Taketa, J. Xu, I. Verpoest *"*Inherent carbon fibre stiffening as seen in textile reinforced composites*"*. In CompTest, Lausanne, 2011.